

SYNTHESIS AND CHARACTERIZATION OF POLYPYRROLE/MAGHNITE NANOCOMPOSITES BY IN SITU INTERCALATIVE POLYMERIZATION

M. A. Zenasni^{1*}, S. Benfarhi², B. Meroufel¹, M. Ragoubi³, A. Merlin³

¹ *Institute of Sciences and Technology, Department of Sciences, Bechar University, BP417 Bechar, 08000 Algeria.*

² *Institute of Sciences, Department of Chemistry, Batna University, 05000 Batna, Algeria.*

³ *Laboratoire d'Etudes et de Recherche sur le MATériaux Bois (LERMAB), EA 4370, University of Lorraine, Nancy, France.*

* am.zenasni@gmail.com

Keywords: Maghnite, Polypyrrole, In situ polymerization

Abstract

MCP nanoclaycomposites based on organoclay modified maghnite (OMag) and polypyrrole polymer (PPy) have been prepared and synthesize in situ intercalative polymerization. Sodium maghnite (Na⁺-Mag) with a cation exchange capacity (CEC) of 101.25 meq/100 g was organically modified (MC) by the intercalation of cetyltrimethylammonium bromide (CTAB).

The nanocomposites were examined by means of XRD, SEM, FT-IR and thermal thermogravimetry/ differential thermal analysis (TG/DTA). Thermal stability of the nanocomposites increased as compared to the pure polymer. It was observed that the spherical shape of the pure polymer beads disappeared on composite formation as evidenced by SEM.

1 Introduction

Over the last decade, considerable attention has been paid to the synthesis and application of clay/polymeric matrix nanocomposites. Polyolefins, i.e. polyethylene and polypropylene, are the most frequently used polymers for clay containing nanocomposites [1–3].

Layered clays such as montmorillonite (MMT) attracted intense research interest for the preparation of polymer clay nanocomposites. These inorganic/organic nanocomposites possess enhanced and novel properties not exhibited by individual inorganic and organic constituents [4–9].

The clay layer is hydrophilic in nature and can be converted to organoclay to promote the wetting of the polymer molecule onto the clay surface [10,11]. By properly controlling the surface properties of the organoclay, various degrees of organoclay dispersion can be achieved to give: (a) conventional composites, (b) intercalated nanocomposites, (c) intercalated-exfoliated nanocomposites and (d) exfoliated nanocomposites [11]. The clay's surface properties can be modified in various ways. One can use clay with a different layer

charge density, control the surfactant surface coverage or vary the kind of intercalated surfactant [12–15].

A polymer, polypyrrole (PPy) (see structure in Figure 1) can be prepared by various methods such as chemical, electrochemical, and vapor phase routes. Angeli et al. [16] first reported the chemical polymerization of pyrrole (Py) monomers in 1916. Miyata and co-workers [17,18] investigated typical chemical synthesis of PPy using anhydrous FeCl_3 as an oxidant/dopant in various solvents. They found that while methanol appeared to be the best solvent for optimal conductivity and morphology, the equilibrium redox potential of the solution controllable via the relative concentration of monomers and oxidants and via addition of FeCl_3 were a more important determinant of polymer quality. The polymer produced in this way showed a more ordered fibrillar morphology and stretched films. Chen et al. [19] also showed that the monomer-to-oxidant ratio determined the electrical conductivity and morphology of the resulting PPy. The high oxidation potential of $\text{FeCl}_3/\text{FeCl}_2$ at a low Py/FeCl_3 ratio can induce the formation of a highly doped PPy, whereas a high Py/FeCl_3 ratio favors the depletion of the oxidant, leading to lower doping levels and lower conductivity. Additionally, degradation of conjugated bonds is possible at a very high FeCl_3 concentration because of the formation of covalent carbon-chloride bonds. Consequently, it was concluded that a maximum conductivity was obtained at a 2:1 monomer to-oxidant ratio.

Recently, the Algerian montmorillonite clay, called Maghnite (Mag), representing a new non toxic cationic initiator, was used as a catalyst for cationic polymerization of a number of vinylic and heterocyclic monomers [20–23].

In the present study, the chemical polymerization method was used to prepared polypyrrole (PPy) in powder form. At both Py/FeCl_3 molar ratios of 5 and 1, the concentration of FeCl_3 was kept constant and methanol was used as a solvent.

The main objective of this work was to find the right surface treatment condition for the 2:1 layer type bentonite from the Maghnia province in Algeria to optimize the organoclay dispersibility in polypyrrole (PPy). Because the source of the clay was fixed, the organoclay surface property was controlled varying the amount of the adsorbed surfactant.

The incorporation of organoclay into polymeric material for large-scale production is often carried out by either in situ intercalative polymerization, where the organoclay is dispersed in a monomer which is subsequently polymerized

In order to determine the composition, size, structural and thermal properties of the nanocomposite several structural investigations viz. X-ray, FT-IR, scanning electron microscope (SEM), and thermogravimetric/differential thermal analysis (TG-DTA) as a function of the annealing temperatures have been carried out and the results are being presented here.

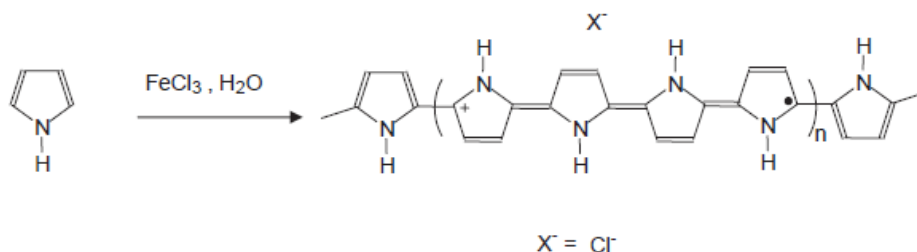


Figure 1. Chemical structure of polypyrrole.

2 Materials and testing methods

2.1 Materials

The maghnite used in this work comes from a quarry located in Maghnia (North West of Algeria) and was supplied by company “ENOF” (an Algerian manufacture specialized in the production of nonferric products and useful substances). The different chemical elements of the native bentonite were transformed into oxides and analysed by Xray fluorescence (ENOF). Results are given in Table 1. These results confirm that the maghnite used consists essentially of montmorillonite, since the ratio $\text{SiO}_2/\text{Al}_2\text{O}_3$ is equal to 3.77 and thus belongs to the family of the phyllosilicates [24]. These maghnites form stable suspensions in water and have flat platelets or needle-like structures. Granulometry of the crude maghnite has been performed in the Civil Engineering Department of Tlemcen University (EDTU) using a sedimentation technique with a 0.1% solution of sodium hexametaphosphate; 95% of the grains were found to have a diameter of less than 100 μm . The cation exchange capacity (CEC) was measured to be 101.25 meq/100 g of clay, and the surface area was 27m²/g, with an average pore size of 7 nm.

Pyrrole (Py) and cetyltrimethylammonium bromide (CTAB) (see structure in table 2) was supplied by Aldrich.

All the solvents were supplied by Aldrich (analytical grade) and used without further purification.

Species	SiO ₂	Al ₂ O ₃	Fe ₂ O ₃	CaO	MgO	Na ₂ O	K ₂ O	TiO ₂	LOI
% (w/w)	65.2	17.25	2.10	1.20	3.10	2.15	0.60	0.20	8.20

Table 1. Chemical composition of the bentonite.

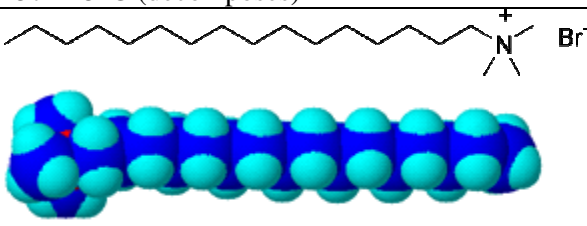
CTAB	
IUPAC Name	hexadecyl-trimethyl-ammonium bromide
Redirected from	cetyltrimethylammonium bromide
Molecular formula	C ₁₉ H ₄₂ BrN
Molar mass (g/mol)	364.45
Appearance	White powder
Melting point	237-243°C (decomposes)
Chemical structure	

Table 2. General properties of CTAB

2.2 Organoclay preparation

The syntheses of maghnite/CTAB organoclays (MC) were performed by the following procedure. 10 g of Na⁺-Mag was dispersed in about 400 ml of distilled water and 3,5g of CTAB was dissolved in 100 ml of distilled water. The concentration of CTAB is 100% of cation exchange capacity (CEC) of Na⁺-Mag was slowly added to stored dispersion of maghnite.

Then, the two solutions were mixed together and stirred for 4 h at 50°C. All products were washed for times with 100ml distilled water, dried at 100°C and ground in an agate mortar to pass through a 200 mesh sieve.

The organoclays were prepared by replacing Na⁺ on the surface of the homoionic clay with either of the one quaternary ammonium cation (CTAB) at 100% of the clay CEC according to the procedure described by Bartelt-Hunt et al. [25]. Briefly, the quantity of organic cation added to the maghnite was determined by equation (1) :

$$f = \frac{M_{\text{cation}}}{\text{CEC} \times M_{\text{caly}} \times \text{GMW}_{\text{cation}} \times Z} \quad (1)$$

Where f is the fraction of CEC satisfied by the organic cation, M_{cation} the mass of organic cation required to achieve the desired fraction of CEC, M_{caly} the mass of the homoionic clay, $\text{GMW}_{\text{cation}}$ the gram molecular weight of the organic cation, and Z is the moles of charge per equivalent.

2.2 Chemical synthesis of polypyrrole

Ppy black powder was synthesized by oxidation of pyrrole (Py) in aqueous solutions containing the adequate oxidants at 25°C for 24h, using urea as a buffer according to the literature [9,26]. The pyrrole was purified by passing through to a column of basic alumina. In summary, 10 g (0.30 mol) pyrrole monomers were dissolved in 400mL distilled water under vigorous stirring. An amount of 6.8 g (0.06 mol) of FeCl₃ (as oxidant) dissolved in 100mL of distilled water was subsequently added drop wise to the previous solution and oxidative polymerization reaction was continued for 24h. The Ppy was formed as precipitate in reaction medium, which was then filtered and washed sequentially with distilled water several times. Finally the product was dried at 60°C.

2.3 Chemical synthesis of polypyrrole/maghnite nanocomposite (MCP)

As a typical experiment for the preparation of PPy/Mag nanocomposite with 10 wt.% clay loading, 1 g organophilic clay (MC) was suspended into 400mL distilled water under magnetic stirring at room temperature. Pyrrole (9 g, 0.13mol) was subsequently added to the above suspension, and kept stirred for 24 h. Afterwards FeCl₃ (6.8 g, 0.06mol) solution in 100mL distilled water, was added and stirred. Nanocomposite material was filtered and washed sequentially with distilled water, methanol, and acetone several times, followed by drying at 60°C [9].

2.4 FTIR, XRD, SEM-EDX and TG-DTA characterizations

The samples of PPy and nanocomposite powder were characterized by using infrared (FT-IR), X-ray diffraction (XRD), X-ray photoelectron spectroscopy (XPS), scanning electron microscopic (SEM) techniques and thermogravimetric-differential thermal analysis (TG-DTA).

The FT-IR absorption spectra are recorded on KBr pressed pellets of the powdered samples in the range 4000-400 cm⁻¹, using a Perkin-Elmer FTIR 1000 spectrophotometer. The X-ray diffraction pattern of powders was recorded on a Phillips-1730 (PANalytical) X-ray diffractometer using Cu K α radiation ($\lambda=1.54\text{\AA}$). TG-DTA thermograms were performed using the multimodule 92-10 Setaram analyser operating from room temperature up to 1000°C in a Al₂O₃ crucible, at 10°C/mn heating rate. The samples were first evaluated using a scanning electronic microscope (MEB HITACHI, S-4800, Berkshire, UK) equipped with an EDX instrument.

3 Results and discussion

3.1 FTIR analysis

FTIR spectrums of the original maghnite and organomaghnite samples are shown in Figure 2 Both the original maghnite (Na⁺-Mag) and the organomaghnite (MC) show characteristic peaks of maghnite. The absorption band at 3650 cm⁻¹ is due to stretching vibrations of structural OH groups of montmorillonite. A complex band at 1050 cm⁻¹ is related to stretching vibrations of Si-O groups. The H₂O-stretching vibration was observed as a broad

band at 3450 cm^{-1} . The spectrum of MC also showed the absorption band at $3000 - 2850\text{ cm}^{-1}$ related to stretching vibrations of C-H groups. However, no more distinct change on the absorption band at $935-450\text{ cm}^{-1}$ in the spectrum of original maghnite. Figure 2 shows KBr pellet FT-IR spectra of PPy, Mag and PPy-Mag nanocomposites. The C=C stretching of the benzene ring appears at 1537 cm^{-1} and the peak at 1292 cm^{-1} is induced by C-N stretching. Strong asymmetric and symmetric S = O stretching bands appeared at 1162 cm^{-1} and 1089 cm^{-1} , respectively. The characteristic peaks of the Si-O, Al-O and Mg-O bonds are appeared in the spectrum of the clay showing bands at 1047 cm^{-1} , 524 cm^{-1} and 468 cm^{-1} , respectively. The characteristic peaks of Maghnite (Mag) clay are present in the spectrum of the nanocomposites, which are clear indications of the presence of clay in the nanocomposites blend. Also the characteristic peak of PPy observed in PPy/Mag nanocomposite systems is a strong evidence of the intercalation of PPy in the nanocomposite systems.

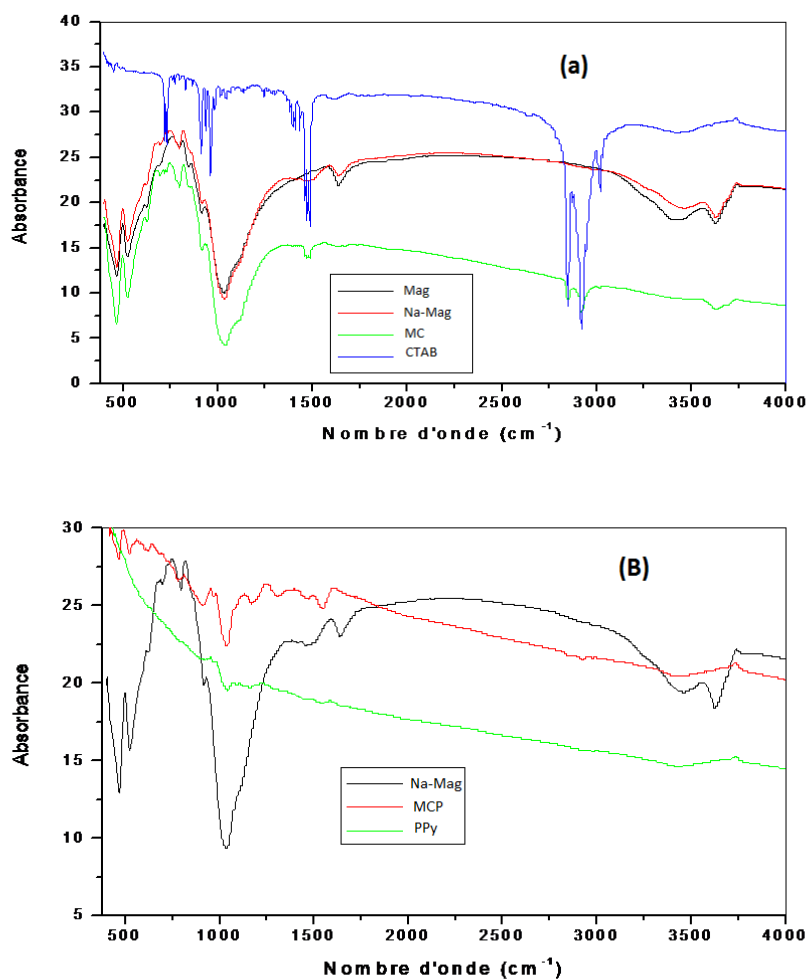


Figure 2. FTIR spectra of MC (a), MCP (b)

3.2 XRD analysis

Intensity loss and disappearance of the clay's XRD base diffraction peak have often been used to indicate that delamination is occurring. However, Gilman et al. have pointed out that XRD analysis alone can lead to false interpretations of the extent of exfoliation [27,28]. Thus, XRD should be applied jointly with TEM analyses. X-ray diffractometry revealed that intercalation was successful with CTAB. The layers were propped open upon swelling in water and the d-spacing became higher after the ion-exchange process by the alkylammonium in comparison

with that of the original clay. Figure 3 shows the XRD patterns of a natural Na⁺-Mag and organoclay (MC) prepared using CTAB and the results are also summarized in Table 3. The d-spacing of unmodified Na⁺-Mag is 1.28 nm calculated from the reflection at 2 θ =7.75°. After the ion-exchange reaction with ammonium salt (CTAB), reflection of the clay shifted to a new position at 2 θ =5.56° (d=2.27nm). An increase of the interlayer distance, leads to a shift of the reflection toward lower angles and confirmed that intercalation and surface modification of Na⁺-Mag had taken place. This means that the basic structures of the Na⁺-Mag is kept, the layers only propped open, and the basal spacing increased significantly (table 3), providing evidence that intercalation has occurred. Insertion of the PPy into the layers of clay is confirmed by XRD measurements, showing alignment of the PPy chains with the layers of clay. Figure 3 also represents XRD patterns of the Na⁺-Mag, PPy and PPy-Mag samples, respectively. The XRD pattern of the PPy indicates an amorphous structure. The crystalline peak at 7.75° in the Maghnite samples corresponds to the periodicity in the direction of (001). The (001) peak was shifted to a lower angle (2 θ = 5.74°) due to the intercalation of PPy material between the clay layers during nanocomposite formation. The variation of d-spacing in direction of the (001) plane was estimated using Bragg formula of $n\lambda=2d \sin \theta$. The d-spacing in direction of (001) plane of the pristine clay samples is 1.28 nm, and that of PPy-Mag is about 1.79 nm. Thus XRD results demonstrate the intercalation of PPy material between the clay layers.

Sample	2 θ (°)	d (001) Spacing (nm)
Maghnite Brute (MB)	7.45	1.55
Maghnite Sodium (Na ⁺ -Mag)	7.75	1.28
Maghnite Modified (MC)	5.56	2.27
Maghnite/PPy (MCP)	5.74	1.79

Table 3. Basal spacing of Na⁺-Mag, organoclays and nanocomposite

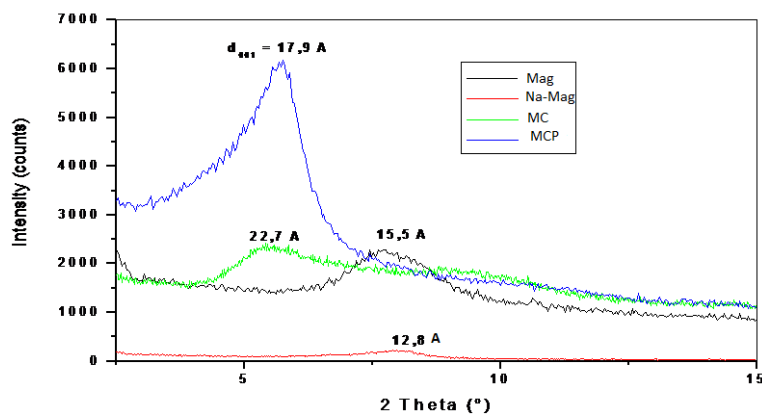


Figure 3. X-ray diffraction spectrum of sodium maghnite (Na-Mag), organomaghnite (MC) and nanocomposite (MCP)

3.3 TG-DTA analysis

The TGA curve for MC is shown in Figure 4. The four-step decomposition known for clay mineral modified with aliphatic organic cation [29,30]. The first step due to loss of residual water trapped in the organoclay starts near 50°C and ends near 150 °C. For the second step corresponding to decomposition of the organic matter (CTAB) present in the organo-

maghnite, the onset occurs near 200°C with two maxima at about 250°C and 380°C. Na⁺-Mag shows much slower decrease in mass in this temperature range. The mass loss in temperature range 200–900 °C increases with the size of the organic cation from 29.22% (MC).

Fig. 4. illustrates the result of the thermo gravimetric analysis of the PPy-Mag (MCP) nanocomposite and pure PPy and Na⁺-Mag. The curve of Na⁺-Mag shows a weight loss of 17.46% below 200°C. In the curve representing pure PPy, the degradation begins at 270°C, moreover the polymer seems to decompose completely by 630°C. While the thermal degradation of the MCP composites all occurs near 260°C, increases for 10°C comparing to pure PPy and is accompanied by two endothermic peaks at 280 and 590°C. The initial mass loss below 125°C attributes to the release of water. The decomposition of the doping anions in PPy begins at 200°C following by a sharp loss in mass from 260°C to 630°C owing to the large-scale thermal degradation of the PPy chains which corresponds to a decrease of 51.7%. Apparently the encapsulated composites increased the thermal stability as PPy layer had better regularity, compaction and continuity. Therefore it can be concluded that the experimental results were in accordance with literatures [31,32].

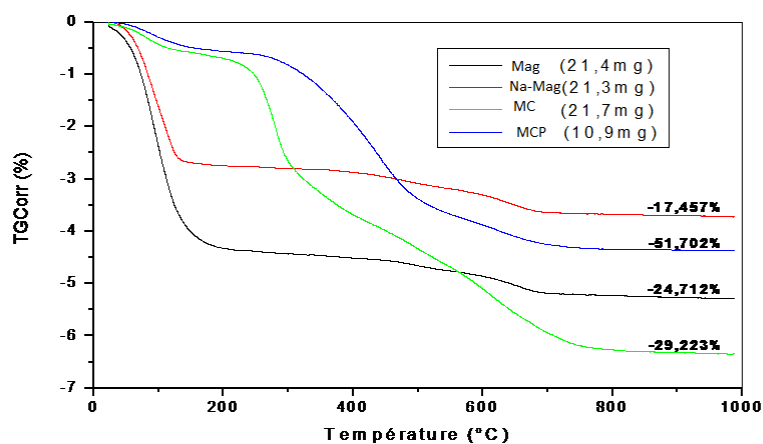


Figure 4. Thermogravimetric analyses of sodium maghnite (Na-Mag), organomaghnite (MC) and nanocomposite (MCP)

3.4 SEM-EDX analysis

The morphology of the MCP nanocomposites is shown in Figure 5. The clay particles were not observed at the surface of MCP. This indicates that during in situ polymerization, clay particles were coated by the polymer, which can be facilitated by an attractive interaction between the PPy and clay surface. PPy is possibly bonded to the surface by hydrogen bonding between the amine groups on PPy chains and the surface oxygen of the clay. Similar interaction between amine group of aniline and the silicate surface in montmorillonite has been reported in Ref. [33].

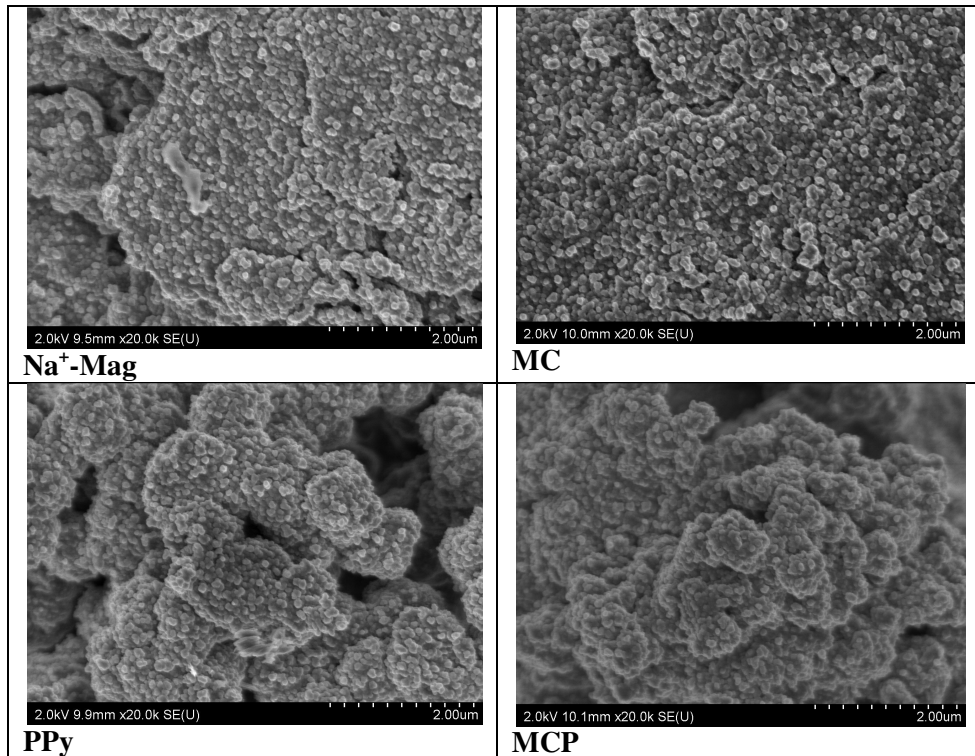


Figure 5. SEM images of Na⁺-Mag, PPy, MC and MCP

The SEM-EDX analyses of the Na⁺-Mag, MC and MCP are shown in Figure 6. The presence of CTAB in maghnite and PPy in MCP nanocomposite could be clearly seen from Figure 6b and c respectively. The presence of CTAB and PPy causes a significant increase in the weight percent for carbon.

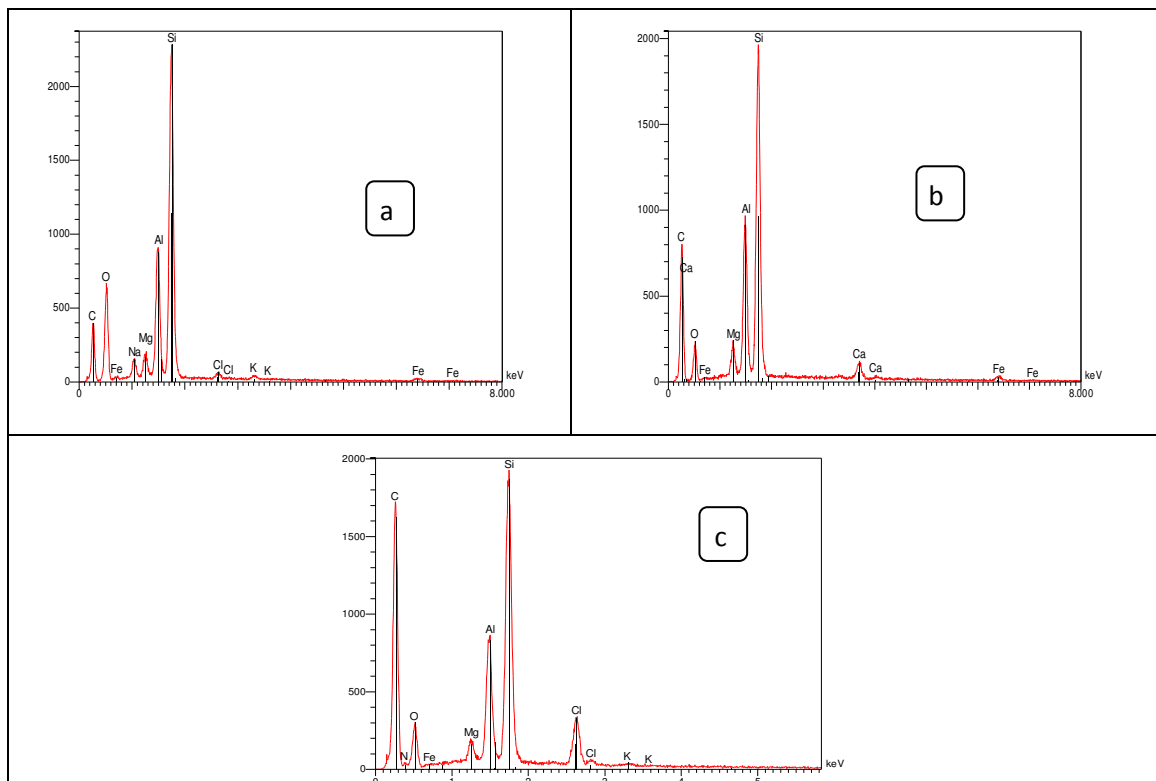


Figure 6. SEM-EDX spectra of (a) Na⁺-Mag, (b) MC and (c) MCP

4 Conclusion

The PPy and MCP nanocomposite were studied by FT-IR and XRD techniques. Also SEM-EDX was used for studying the morphology of maghnite sodic (Na⁺-Mag), Modified maghnite by CTAB (MC) and Polypyrrole/modified Maghnite (MCP), blends.

SEM images allowed for closer look at the morphology of MCP revealing that the PPy is definitely finding its way into clay galleries as suggested by XRD.

Acknowledgements

The authors wish to thank Dr Mohamed CHEHIMI of ITODYS laboratory, University of Paris 7 for the thermogravimetric, DRX and FT-IR analysis and Joint Service Electronic Microscopy and Microanalysis at the University Henri Poincaré of Nancy for MEB-EDX analysis

References

- [1] Suprakas Sinha Ray., Masami Okamoto. Polymer/layered silicate nanocomposites: a review from preparation to processing. *Prog. Polym. Sci.*, **28**, pp. 1539–1641 (2003).
- [2] Alexandre M., Dubois P. *Mater. Sci. Eng.* **28**, (2000).
- [3] Garcia-Lopez D., Picazo O., Merino J.C., Pastor J.M., *Eur. Polym. J.* **39**, pp. 945 (2003).
- [4] Lepoittevin B., Pantoustier N., Devalckenaere M., Alexandre M.L., Kubies D., Calberg C., Jerome R., Dubois P., *Macromolecules*, **35**, pp. 8390 (2002).
- [5] Messersmith P.B., Giannelis E.P., *Chem. Mater*, **5**, pp. 1064 (1993).
- [6] Vaia R.A., Ishii H., Giannelis E.P., *Chem. Mater*, **5**, pp. 1694 (1993).
- [7] Vaia R.A., Giannelis E.P., *Macromolecules*, **30**, pp. 8000 (1997).
- [8] Maiti P., Hoai Nam P., Okamoto Naoki Hasegawa M., Usuki A., *Macromolecules*, **35**, pp. 2042 (2002).
- [9] Hosseini M.G., Raghibi-Boroujeni M., Ahadzadeh I., Najjar R., Seyed Dorraji M.S., Effect of polypyrrole–montmorillonite nanocomposites powder addition on corrosion performance of epoxy coatings on Al 5000. *Progress in Organic Coatings*, **66**, pp. 321–327 (2009)
- [10] Lu C., Mai Y.W., Influence of aspect ratio on barrier properties of polymer–clay nanocomposite. *Phys. Rev. Lett.*, **95**, pp. 88303–88306 (2005).
- [11] Dennis H.R., Hunter D.L., Chang D., Kim S., White J.L., Cho J.W., Paul D.R., Effect of melt processing conditions on the extent of exfoliation in organoclay-based nanocomposite. *Polymer*, **42**, pp. 9513–9522 (2001).
- [12] Osman M.A., Ploetzeb M., Suter U.W., Surface treatment of clay minerals—thermal stability, basal-plane spacing and surface coverage. *J. Mater. Chem.*, **13**, pp. 2359–2366 (2003).
- [13] Osman M.A., Ernst M., Meier B.H., Suter U.W., Structure and molecular dynamics of alkane monolayers self-assembled on mica platelets. *J. Phys. Chem. B*, **106**, pp. 653–662 (2002).
- [14] Xie W., Gao Z., Liu K., Pan W.P., Vaia R., Hunter D., Singh A., Thermal characterization of organically modified montmorillonite, *Thermochim. Acta*, **367-368**, pp. 339–350 (2001).
- [15] Hoshino J., Limpanart S., Khunthon S., Osotchan T., Traiphol R., Srikhirin T., Adsorption of single-strand alkylammonium salts on bentonite, surface properties of the modified clay and polymer nanocomposites formation by a two-roll mill. *Materials Chemistry and Physics*, **123**, pp. 706–713 (2010).
- [16] Angeli A., Alessandri L., *Gazz. Chim. Ital.*, **46**, pp. 283 (1916).

- [17] Waghuley S.A., Yenorkar S.M., Yawale S.S., Yawale S.P., Application of chemically synthesized conducting polymer-polypyrrole as a carbon dioxide gas sensor. *Sensors and Actuators B*, **128**, pp. 366–373 (2008)
- [18] Whang Y.E., Han J.H., Nalwa H.S., Watanabe T., Miyata S., Chemical synthesis of highly electrically conductive polymers by control of oxidation potential. *Synth. Met.*, **41–43**, pp. 3043–3048 (1991).
- [19] Chen X., Devaux J., Issi J.P., Billaud D., Chemically oxidized polypyrrole: Influence of the experimental conditions on its electrical conductivity and morphology. *Polym. Eng. Sci.*, **35**, pp. 642–647 (1995).
- [20] Gherras H., Hachemaoui A., Yahiaoui A., Benyoucef A., Belfedal A., Belbachir M., Chemical synthesis and characterization of a new soluble conducting polymer. *Synthetic Metals*, (2012) *article in press*.
- [21] Yahiaoui A., Belbachir M., *J. Appl. Polym. Sci.*, **100**, pp. 1681–1687 (2006).
- [22] Hachemaoui A., Yahiaoui A., Belbachir M., *J. Appl. Polym. Sci.*, **102**, pp. 3741–3750 (2006).
- [23] Meghabar R., Megherbi A., Belbachir M., *Polymer*, **44**, pp. 4097–4100 (2003).
- [24] Zenasni M.A., Benfarhi S., Meroufel B., Effect of the Degree of Ionization on the Insertion of Polyvinylpyridinium Salts into Bentonite. Hindawi Publishing Corporation, *International Journal of Inorganic Chemistry*, **Volume 2011**, Article ID 723020, 6 pages
- [25] Bartelt-Hunt S.L., Burns S.E., Smith J.A., Nonionic organic solute sorption to two organobentonites as a function of organic-carbon content. *J. Colloid Interface Sci.*, **266**, pp. 251–258 (2003).
- [26] Abel M.L., Chehimi M.M., *Synth. Met.*, **66**, pp. 225 (1994).
- [27] Morgan A.B., Gilman J.W., Jackson C.L., *Proceedings of ACS division of polymeric materials science and engineering*. San Francisco, CA., Washington, DC: American Chemical Society, 82, pp. 270 (2000).
- [28] Morgan A.B., Gilman J.W., *J Appl Polym Sci*, **87**, pp. 1329–38 (2003).
- [29] Xi Y., Ding Z., He H., Frost R.L., Structure of organoclays an x-ray diffraction and thermogravimetric analysis study. *J. Colloid Interface Sci.* **277**, pp. 116–120 (2004).
- [30] Jankovič L., Madejová J., Komadel P., Jochech-Mošková D., Chodák I., Characterization of systematically selected organo-montmorillonites for polymer nanocomposites. *Applied Clay Science*, **51**, pp. 438–444 (2011).
- [31] Pojanavaraphan T., Magaraphan R., Fabrication and characterization of new semiconducting nanomaterials composed of natural layered silicates (Na⁺-MMT), natural rubber (NR), and polypyrrole (PPy). *Polymer*, **51**, pp. 1111–1123 (2010).
- [32] Pourabbasa B., Pilati F., Polypyrrole grafting onto the surface of pyrrole-modified silica nanoparticles prepared by one-step synthesis. *Synthetic Metals*, **160**, pp. 1442–1448 (2010).
- [33] Yariv S., Heller L., Kaufherr N., *Clay Miner*, **301**, pp. 301–308 (1969).